We are IntechOpen, the world's leading publisher of Open Access books Built by scientists, for scientists

4,800
Open access books available

122,000
International authors and editors

135M
Downloads

Our authors are among the

154
Countries delivered to

TOP 1%
most cited scientists

12.2%
Contributors from top 500 universities

CLARIVATE ANALYTICS BOOK CITATION INDEX INDEXED

WEB OF SCIENCE™

Selection of our books indexed in the Book Citation Index in Web of Science™ Core Collection (BKCI)

Interested in publishing with us?
Contact book.department@intechopen.com

Numbers displayed above are based on latest data collected.
For more information visit www.intechopen.com

12

Fluid Pressurization in Cartilages and Menisci in the Normal and Repaired Human Knees

LePing Li and Mojtaba Kazemi
University of Calgary
Canada

1. Introduction

Computer simulation has found extensive applications in biomedical engineering. In particular, finite element methods have been used in orthopaedic biomechanics to help design prostheses and implants and understand joint injuries and diseases. We are interested in the mechanics of the knee joint that is associated with the fluid pressure and flow in the articular cartilages and menisci. This section presents a brief review of current status of computer mechanical modeling of the human knee and the cartilaginous tissues. The background of our present research will be understood in this section.

1.1 Mechanical structure of the knee

The human knee joint is a complex mechanical structure. It connects the two major bones of the lower limb together: the femur and tibia. Femoral and tibial cartilages, which are hydrated soft tissues, cover the ends of the femur and tibia respectively (Fig. 1, finite element model). These articular cartilages together with menisci, another hydrated soft tissue, provide smooth articulating surfaces that redistribute the joint loading and reduce stress concentrations in the bones. The lubrication in the knee is provided by the synovial fluid and low stiffness of the cartilaginous tissues, including cartilages and menisci. During daily activities such as walking and running, a normal knee experiences minimum frictions and virtually no wear (Callaghan et al., 2003; Swanson, 1979). The femoral cartilage has a curved shape while the tibial cartilages are almost flat. The two menisci locate between the femoral and tibial cartilages and provide the shape congruency in the knee joint. Each meniscus has a crescent-like form, and is connected to the tibia plateau at the both ends by meniscus horns. The wedge-shape cross-section of the menisci minimizes the direct contact of the femoral and tibial cartilages. In the case of healthy menisci, the direct contact can be as low as 10% of the cartilage surfaces (Walker & Erkman, 1975). By improving the joint congruency, the menisci support and redistribute the joint load, increase the joint stability and facilitate lubrication (Fithian et al., 1990; Kurosawa et al., 1980; Walker & Hajek, 1972). Ligaments are fibrous tissues with fibers mainly aligned in the longitudinal direction. Four ligaments connect the femur and tibia or fibula. They are Medial Collateral Ligament (MCL), Lateral Collateral Ligament (LCL), Anterior Cruciate Ligament (ACL) and Posterior Cruciate Ligament (PCL). Among the main roles of ligaments is to stabilize the joint and support a portion of the applied load (Daniel et al., 1990). Other important mechanical components include tendons and muscles, which are beyond the scope of this chapter.

The main constituents of the cartilage and menisci are fluid, collagen fibers (mainly type II in cartilages and type I in menisci) and proteoglycan matrix. The fluid is the most abundant component of these tissues. It takes 68-85% of the weight of cartilage and 60-70% of the menisci (Mow & Ratcliffe, 1990). Hydrated tissues such as cartilages and menisci are viscoelastic: they exhibit stress relaxation when the strain is held constant and creep when the stress is held constant. The viscoelastic behavior is mainly due to the interstitial fluid flow and the intrinsic viscoelasticity of the collagen fibers. In general, cartilaginous tissues appear very soft to facilitate joint movement when they are not pressurized. However, under fast knee compressions, these tissues can be highly pressurized to support and redistribute loadings (Mow et al., 1980; Spilker et al., 1992).

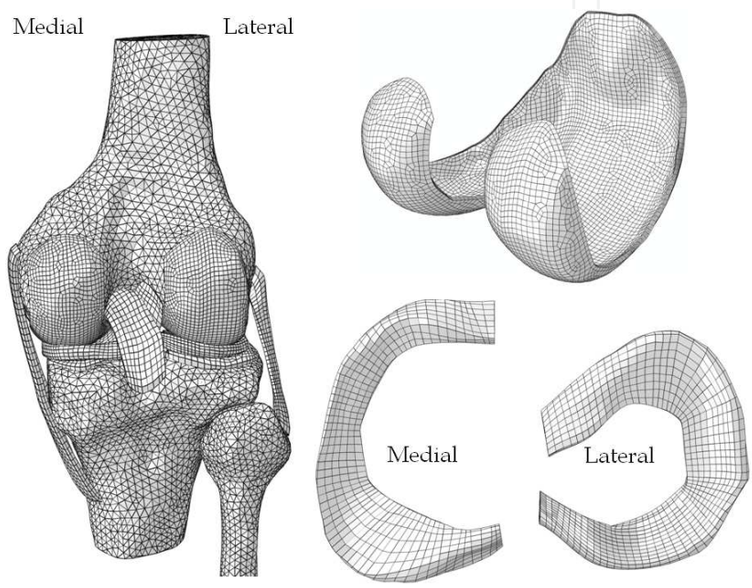

Fig. 1. Finite element model of the knee joint. Top right: femoral cartilage (posterior view); bottom right: menisci (top view). The model was obtained from a young male's right knee (the patella was not modeled)

The mechanical function of the knee joint is partially performed through mechanical contacts between several contacting pairs of cartilaginous tissues. The major contact pairs are the femoral cartilage–tibial cartilage, femoral cartilage–menisci and menisci–tibial cartilages. Understanding the contact mechanics of the individual knee tissues as well as the whole joint assembly may lead to better prevention, diagnosis and treatment of joint injury and diseases. The changes in the health state of the cartilages or menisci can alter the contact mechanics of the knee and therefore affect its normal functioning. For instance, partial meniscectomy, which is a surgical operation to remove the injured part of the meniscus, can alter the stress and pressure distributions in the cartilaginous tissues and may initiate or advance osteoarthritis.

1.2 Finite element modeling of the knee

Finite element methods have been extensively used to investigate the mechanics of the knee joint or its individual tissues. The advantages of using finite element simulations compared to the experimental studies include convenient control of load and boundary conditions,

easy evaluation of stress and strain fields, time and cost efficiency and capability of parametric studies. However, each finite element study is associated with numerous simplifications in geometrical modeling, material definition, constitutive behavior, etc. In recent two decades, new finite elements have been proposed to improve modeling and eliminate some limitations. Simplified or experimental explants geometries have been widely used to validate the complex constitutive relationships of the knee tissues. Earlier joint modeling was also based on axisymmetrical or plane-strain geometries: two pieces of tissues in two dimensional geometries were often used to represent a knee joint contact (Adeeb et al., 2004; Wu et al., 1998). More recently, anatomically accurate knee models become increasingly popular for the investigation of realistic joint contact in different loading conditions and health states. These real knee geometries are normally reconstructed from the Computer Tomography (CT) or Magnetic Resonance Imaging (MRI). The constitutive modeling used for the hydrated soft tissues may be classified into three main categories: *single-phase* solid models, *poroelastic* or *biphasic* models (with additional fluid phase) and *fibril-reinforced* models (fluid phase and fibril-reinforced solid phase). Due to time cost and convergence difficulties associated with the anatomically accurate models, simpler constitutive behaviors (commonly single-phase) have been used in these studies as compared to the cases with simplified geometries.

1.3 Constitutive modeling of the knee tissues

The finite element studies of articular cartilage and menisci have been quite comprehensive with experimental tissue testing geometries (Ateshian et al., 1994; Li et al., 2003; Mow et al., 1980). The constitutive models used in these studies have been evolved from that for single-phase materials, i.e. from that for a structural steel (Coletti et al., 1972; Hayes et al., 1972; Kempson et al., 1971). Since only elastic properties were considered in the single-phase material, the time dependent load response resulted from the fluid flow could not be described by these early models. Linear elasticity, homogeneity and isotropy were often assumed (Armstrong et al., 1980; Hayes et al., 1972). Some single-phase models featured viscoelastic behavior using dashpots and springs (e.g. Kelvin-Voigt-Maxwell models). They had the potential to describe the time dependent responses (Coletti et al., 1972; Hayes & Mockros, 1971; Parsons & Black, 1977). However, the fluid flow relative to the tissue matrix could not be described by such modeling. Another limitation was associated with the use of effective modulus, when a single-phase elastic model was employed. Instead of the real Young's modulus of the tissue matrix, a greater effective modulus accounting for the stiffness of the pressurized tissue had to be used, in order to match the stress measured experimentally. This effective modulus is generally pressure-dependent, resulting in uncertainties in its appropriate determination and thus uncertainties in the results (Li and Gu, 2011).

Poroelastic/biphasic models for biological tissues were proposed to capture the time dependent response of the tissues (solid + fluid phases). Poroelastic models were based on the soil consolidation theory (Biot 1941, 1962), while the biphasic theory was initially proposed by Mow et al. (1980) using the theory of porous media. It was believed that these two theories yield similar results if the fluid was assumed as inviscid (Simon, 1992). In fact, it was shown that the linear poroelasticity was essentially equivalent to the linear theory of porous media, although some inconsistencies were observed in correlating the material properties (Schanz and Diebels, 2003). The early poroelastic models were developed to

investigate the mechanics of bones (Nowinski, 1971, 1972; Nowinski and Davis, 1970, 1972). The biphasic models have been improved substantially from its initial linear version (Mow et al., 1980), e.g. variable permeability (Lai et al., 1981) and large deformation have been formulated (Suh et al., 1991). Many independent formulations were also developed (e.g. Lanir, 1987). The biphasic models were found to be able to account for the mechanical response of articular cartilage at low strain-rates only (Brown and Singerman, 1986; Miller, 1998).

The load response of articular cartilage is highly transient. Given a compression, the stress in the tissue can be an order higher at a high compression rate than that at a low compression rate (Oloyede et al., 1992). Fibril-reinforced models were proposed to capture this high-ratio of fast versus slow compressions. In a fibril-reinforced model, the solid phase was separated into two constituents: the fibrillar and non-fibrillar matrices. The non-fibrillar matrix defines the proteoglycan matrix, and the fibrillar matrix models the collagen network (Soulhat et al., 1999). It was found that the nonlinear fibrillar properties must be considered in order to account for the strong transient responses of articular cartilage (Li et al. 1999b). In a finite element procedure, the fibrillar matrix could be represented by discrete spring elements (Li et al. 1999b; Soulhat et al., 1999) or continuum elements (Li & Herzog, 2004; Wilson et al., 2004). A fibril-reinforced model was used for the soft tissues in the present study.

1.4 Anatomically accurate knee modeling

Poroelastic and fibril-reinforced models have been extensively used to describe the tissue mechanical behavior for the problems with simple geometries. However, these studies have not been extended to the anatomically accurate knee models until our recent work (Gu and Li, 2011). Single-phase material models have been commonly used in the joint finite element modeling. The geometrical data of these models were commonly obtained from CT and MRI. A typical finite element model of the tibio-femoral joint is illustrated in Fig. 1. In many three-dimensional models, bones are considered as rigid due to their higher stiffness compared to the soft tissues (3 orders in difference). The fluid pressure in the soft tissues is normally ignored to avoid the numerical difficulties resulted from complicated mechanical contacts and time-dependent responses (Bendjaballah et al., 1995; Li et al., 1999a; Peña et al., 2005). Articular cartilages were often simplified as single-phase, linear elastic, homogenous and isotropic materials (Haut Donahue et al., 2002; Peña et al., 2006). Menisci were modeled as isotropic (Peña et al., 2005, 2006, 2008), transversely isotropic (Haut Donahue et al., 2002) or fiber-reinforced linearly elastic solid (Penrose et al., 2002; Shirazi et al., 2008). Example case studies are: knee joint under compression (Bendjaballah et al., 1995; Shirazi et al., 2008), knee joint in combined loading (Peña et al., 2006; Shirazi & Shirazi-Adl, 2009), effect of meniscectomies (Peña et al., 2005, 2008; Yang et al., 2009; Zielinska & Donahue, 2006) and effect of ligament reconstruction on the knee joint biomechanics (Shirazi & Shirazi-Adl, 2009; Suggs et al., 2003).

Although fluid flow is believed to play a substantial role in the load response of the knee, little information is known about the fluid pressurization in cartilages and menisci in the real knee contact configuration. By modeling the fluid flow in the soft tissues, the time dependent response of the knee joint can be described, i.e. the creep and relaxation behaviors can be predicted. Further important information may be obtained. For instance, not only the magnitude, but also the distribution of contact pressure between the articular

surfaces was found to be different when the fluid pressure was modeled (Li and Gu, 2011). The location of the maximum contact pressure may also change with creep or relaxation, which cannot be predicted by a single-phase elastic model. Mechanical response associated with fluid pressurization in the tissues may play important roles in the scenarios previously studied, which might not have been understood because the fluid pressure was ignored. Considering the difficulties associated with in-situ measurements of fluid pressure in cartilage and menisci, a three-dimensional computational model is a good option for the determination of the fluid pressurization in these tissues. The fluid flow has been successfully modeled in a three-dimensional fiber-reinforced model of the temporomandibular joint (Perez del Palomar & Doblare, 2007). More recently, a three-dimensional anatomically accurate knee model has been proposed to capture the stress relaxation and creep behaviors of the healthy and meniscectomized knee joints (Gu & Li, 2011; Kazemi et al., 2011, Li and Gu, 2011). We will consider some complementary results here.

2. Methods

The mechanical responses were simulated for the intact knee, as well as six cases of partial meniscectomy at different sites. The finite element modeling developed in our previous studies will be briefly reviewed in this section. The meshes, material properties and loading conditions for the present study will be particularly discussed.

2.1 Geometry and finite element mesh

The joint geometry was obtained using the Magnetic Resonance Imaging (MRI) of a healthy male's right knee in full extension (Cheung et al., 2005). The commercial finite element software ABAQUS v6.8-2 (Simulia Inc., Providence, RI, USA) was used to generate the mesh (Fig. 1). The model consisted of the distal femur, tibia, fibula, articular cartilages, menisci and the four major ligaments (ACL, PCL, MCL and LCL). Bones were considered as rigid and triangular elements were used to mesh their surfaces (triangles normally describe a curved surface better). In total, 12,829 surface elements were used for the bones (Table 1).

Tissue	Femur	Tibia	Fibula	Femoral cartilage	Tibial cartilage	Menisci	ACL	PCL	LCL	MCL
Number of elements	5668	5385	1776	18432	637	3423	288	306	456	516
Number of nodes	2836	2709	891	89689	1482	5117	513	540	780	924

Table 1. Nodes and elements for individual tissues in the finite element mesh of the knee

Articular cartilages, menisci and ligaments were meshed using hexahedral elements. Porous elements with linear variation of fluid pressure and quadratic variation of displacement were chosen for the femoral cartilage (20 nodes). Porous elements with linear variation of displacement were used for the menisci and tibial cartilages (8 nodes). Solid elements with linear displacement were used for the ligaments. In total, 24,058 elements and 99,045 nodes were used to mesh the soft tissues of the healthy knee (Table 1).

In order to model the total and partial meniscectomized knees, the elements corresponding to the resected meniscus were removed from the intact element assembly. Here, the total meniscectomy refers to the complete removal of both medial and lateral menisci. For the partial meniscectomy, two sites of resections in the avascular zone (inner peripheral meniscus) were considered. One resection was in the lateral and one in the medial meniscus. They were thus referred as to the extended lateral meniscectomy and extended medial meniscectomy, respectively. Meniscectomies in this zone are more common because lesions there have very low chance of natural healing due to absence of blood supply in the zone. The resection is often longitudinal or in the circumferential direction (Dandy, 1990; Greis et al., 2002). An extended meniscectomy encountered longer resection in the longitudinal direction.

2.2 Material properties

Cartilages, menisci and ligaments were modeled as fibril-reinforced materials. The fiber orientation in the femoral cartilage was assumed based on the split line patterns (Below et al., 2002). For the menisci, the primary fibers were oriented circumferentially (Aspden et al., 1985). The fibers in the tibial cartilage were oriented randomly due to lack of information about the primary fiber direction in this tissue. In the case of ligaments, the fibers were aligned in the longitudinal direction. The initial strains in ligaments were ignored since only small deformation was considered in the current study. The reported initial strains of the ligaments are normally beyond the small deformation range (Grood & Hefzy, 1982).

The non-fibrillar matrix of the soft tissues was considered as linearly elastic and isotropic. The viscoelasticity of collagen fibers was formulated previously (Li et al., 2009) but omitted here in favor of brevity. In short, the following relation was used for the fibrillar stiffness in the primary fiber direction, x:

$$E_x^f\left(\varepsilon_x\right) = E_x^0 + E_x^\varepsilon \varepsilon_x \tag{1}$$

where ε_x is the tensile strain, and E_x^0 and E_x^ε are elastic constants in x direction. The same equations, but with different values for coefficients, were used for the y and z directions. The compressive stiffness of the fibrillar matrix was ignored.

The fibrillar properties of different tissues were determined from previous fibril-reinforced modeling and experimental data from the literature (Hirokawa & Tsuruno, 2000; Li et al., 2003; Shirazi et al., 2008; Woo et al., 1976). The numerical values of material properties are listed in Table 2. More details and references about the material properties can be found in our recent papers (Gu and Li, 2011; Kazemi et al., 2011).

2.3 Contact interactions

Cartilaginous tissues in the knee are in multiple mechanical contacts between the mating surfaces. These contacts require particular attention for a successful simulation. For each contact pair, one surface is selected as the master surface and the other one as the slave surface. A master surface may penetrate the mating slave surface, but the other way is not permissible. The surface discretization can be node-to-surface or surface-to-surface. The contact constraint can be enforced with different methods. The efficiency of a contact enforcement method is usually determined by the type of surface discretization. In the present study with the existence of fluid pressure in three-dimensional geometries, surface-to-surface discretization was selected and the linear penalty method was found to be the most efficient approach for the contact enforcement.

Tissues	Fibrillar elastic moduli (MPa), Eq. (1)				Non-fibrillar solid matrix			
	Primary fiber direction x		Directions y & z		Young's modulus (MPa)	Poisson's ratio	Permeability (mm^4/Ns)	
	E^0	E^ε	E^0	E^ε			Direction x	Directions y & z
Femoral cartilage	3	1600	0.9	480	0.26	0.36	0.002	0.001
Menisci	28	0	5	0	0.50	0.36	0.002	0.001
Tibial cartilage	2	1000	2	1000	0.26	0.36	0.002	0.001
Ligament	10	14000	0	0	1.0	0.30	0	0

Table 2. Material properties of the soft tissues used in the finite element simulation

For the intact and partially meniscectomized knees, six contact pairs were defined (three on the medial and three on the lateral side): femoral cartilage-tibial cartilage, femoral cartilage-menisci and menisci-tibial cartilage. Obviously, for the total meniscectomy, only contacts between the femoral and tibial cartilages remained (2 pairs). Frictional contact with a coefficient of 0.02 (Mow et al., 1993) was considered for all the contacts.
The ends of the ligaments and menisci were TIED (fixed) to the bones at the insertion sites. This is obviously in agreement with the actual attachment of the ligaments to the bones. The ends of meniscus are actually fixed to the tibia through meniscus horns. The horns were not particularly modeled in the present study.

2.4 Loads, boundary conditions and solution methods

A stress relaxation protocol was used for the study of the intact, partial and total meniscectomized knees. For the purpose of comparison, the loading and boundary conditions were chosen to be as close as possible to that of similar experimental studies. In all cases, a ramp knee compression of 0.3 mm was applied in one second and remained constant thereafter. The displacement was applied to the femur in proximal-distal direction. Femur was free in all translations but fixed in all rotations. In all cases, the knee joint was assumed in full extension and the tibia and fibula were constrained in all directions.
A complete description of the solution methods is beyond the scope of this chapter. The overall procedure is presented here briefly. More details can be found in our recent papers (Gu and Li, 2011; Kazemi et al., 2011) and the ABAQUS manuals. The implicit finite element method with transient *Soil Consolidation* option available from ABAQUS/Standard was used for the current study. The Newton method was chosen to solve the nonlinear equations. In each iteration of a typical time increment, the convergence of force and volumetric flux was checked at first. In an iteration with converged force and volumetric flux, the convergence of displacement and fluid pressure was assessed. If the convergence of force, volumetric flux,

displacement and fluid pressure was satisfied, the final convergence was accepted when the largest increment in fluid pressure was less than a given value (5 kPa in all cases presented here).
The computer simulations were done on the high performance computers at the University of Calgary (Westgrid) and on our Dell workstations (4 CPUs with 16 GB RAMs). It took a week or two to complete one simulation.

3. Results

Most of the results were plotted for the times 1 and 2000 seconds. The knee compression reached its maximum of 0.3 mm at 1 second followed by relaxation. At 2000 second, the fluid pressure was greatly reduced for the relaxation loading protocol considered (this time may not be long enough for substantial pressure reduction in other cases).

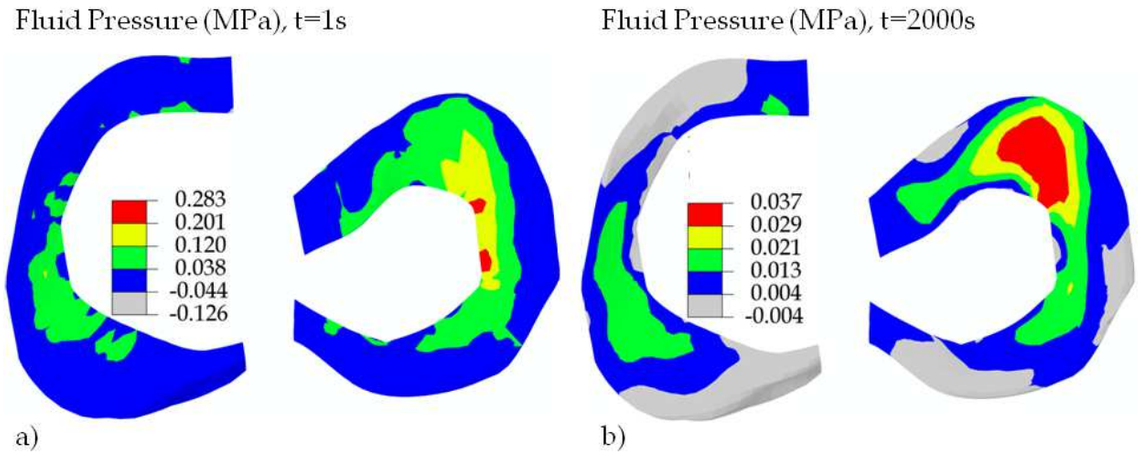

Fig. 2. Fluid pressure in the menisci of an intact right knee. The pressure was obtained for the centroids of the elements. The lateral meniscus is on the right with the posterior side shown in the lower part in each figure (top view)

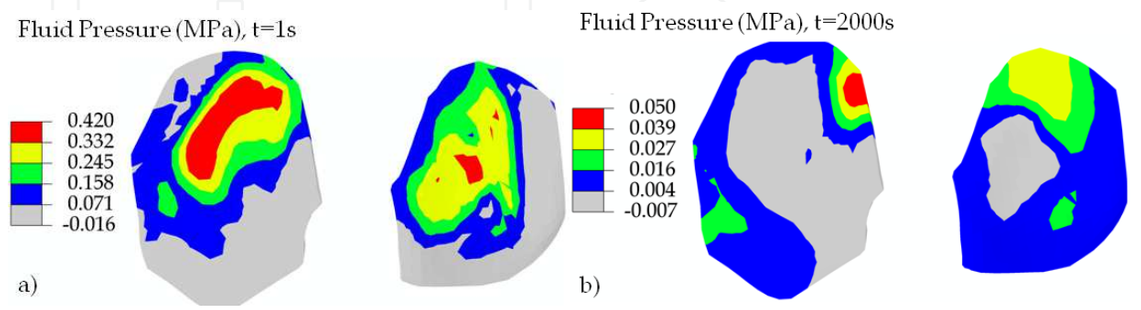

Fig. 3. Fluid pressure in the tibial cartilages of the intact knee. The pressure was obtained for the centroids of the elements. The lateral side is on the right (top view)

NORMAL KNEE − Selected results for the intact joint are shown in Figs. 2-6. The lateral meniscus, which is on the right in Fig. 2a or 2b, was more pressurized than the medial one. The high-pressure region moved toward the anterior side with relaxation (Fig. 2b). The tibial

cartilage, on the other hand, was more pressurized on the medial side (Fig. 3). The short-term contact pressure on the articular surface of the tibial cartilage, which could be in contact with the femoral cartilage and menisci, was consistent with the fluid pressure (Figs. 4a vs 3a). A bigger difference in pattern between the fluid and contact pressures was observed at 2000 second (Figs. 4b vs 3b), because the fluid pressure was less significant at later times.

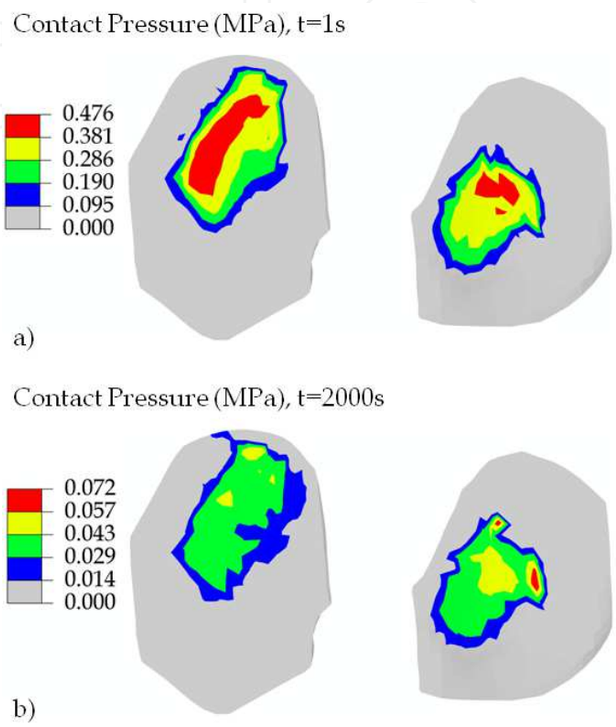

Fig. 4. Contact pressure on the articular surface of the tibial cartilages for the intact knee. The lateral side is on the right (top view)

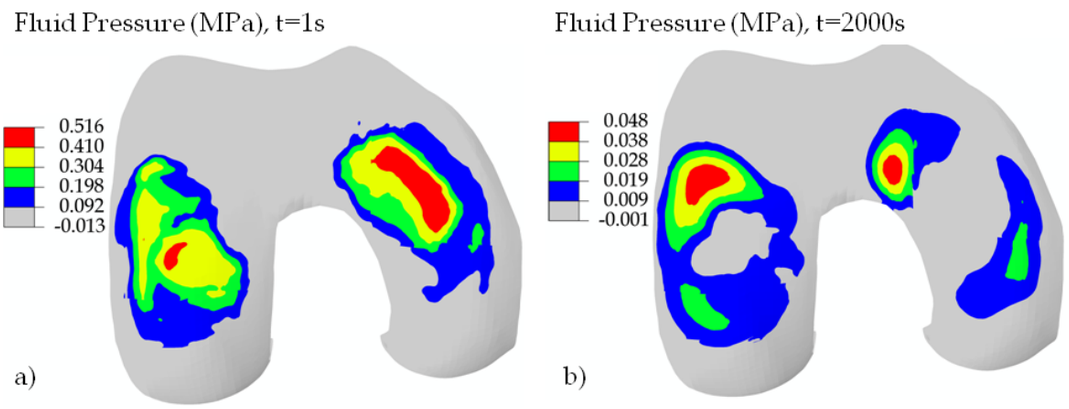

Fig. 5. Fluid pressure in the deep layer of the femoral cartilage for the intact knee. The pressure was obtained for the centroids of the elements that were located approximately 3/4 of the depth from the articular surface. The medial condyle is on the right (inferior view)

The fluid pressure contour for the deep layer of the femoral cartilage (Fig. 5) shows a more regular pattern than that for the menisci (Fig. 2), possibly indicating better results. This was probably because the mesh for the femoral cartilage was more refined, and the mesh for the menisci was mostly irregular due to the wedge shape of the menisci. The contact pressure on the articular surface of the femoral cartilage (Fig. 6) had some similarities with the fluid pressure (Fig. 5), but the differences in distribution are clearly seen. One can also see that the contact pressure in the knee was mainly contributed by the fluid pressurization, because it was decreased substantially with relaxation (Fig. 6b vs 6a).

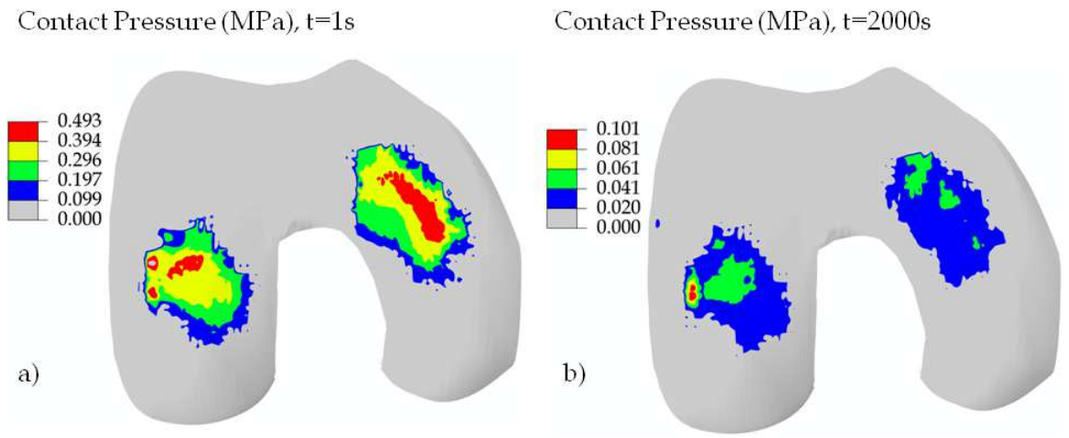

Fig. 6. Contact pressure on the articular surface of the femoral cartilage for the intact knee. The medial condyle is on the right (inferior view). The colors do not show the contact areas exactly, because each color stands for a range of contact pressure. In particular, the color grey does not mean precisely zero pressure there.

It should be noted that all results presented here were obtained using the small deformation assumption. The compression of 0.3 mm was not a physiological loading. The maximum pressures shown in Fig. 6 is merely 10% of possible maximum pressure. The high-pressure regions may be altered if large compression is applied.

PARTIAL MENISCECTOMY − The contact mechanics of the knee was also investigated previously for six cases of partial meniscectomies. In that study (to be published), creep loading protocols were considered. We consider the relaxation loading here for two cases only, the extended lateral and medial meniscectomies. The effect of partial meniscal resections on joint mechanics was more significant in these two cases (Figs. 7-10).

The fluid pressures in the menisci for the two cases of partial meniscectomies were preliminary (Fig. 7). No substantial differences were observed for the two cases (although some small differences are shown in Fig. 7, as comparing Figs. 7a with 7c and 7b with 7d). It was not clear whether this was due to the inaccuracy of the mesh for the menisci or due to

small compression applied to the knee. For the same two cases, however, significantly different fluid pressures were observed in the tibial cartilages (Fig. 8). The higher fluid pressure occurred at the side where the meniscus was partially removed. Furthermore, the maximum fluid pressure was much greater in the case of extended medial meniscectomy (Fig. 8c,d) than that in extended lateral meniscectomy (Fig. 8a,b). This was the case because the higher pressure should have occurred on the medial side even for the intact knee. Now, the meniscectomy on this side made it worse with higher pressurization (Fig. 8, lower figures compared to the upper figures respectively).

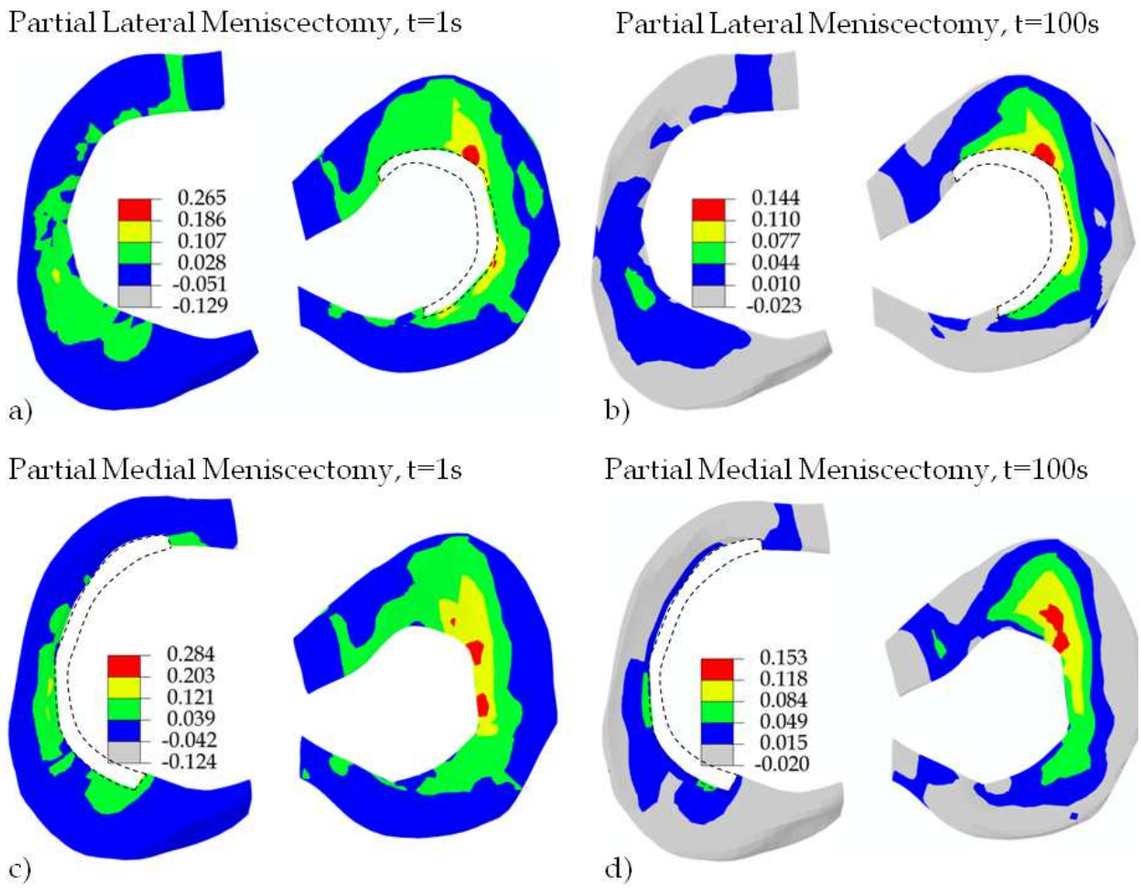

Fig. 7. Fluid pressure (MPa) in the menisci of partial meniscectomized knees. (a) and (b) extended lateral meniscectomy; (c) and (d) extended medial meniscectomy. The lateral meniscus is on the right with the posterior side shown in the lower part in each figure (top view). The sites of resection are indicated with the dashed lines.

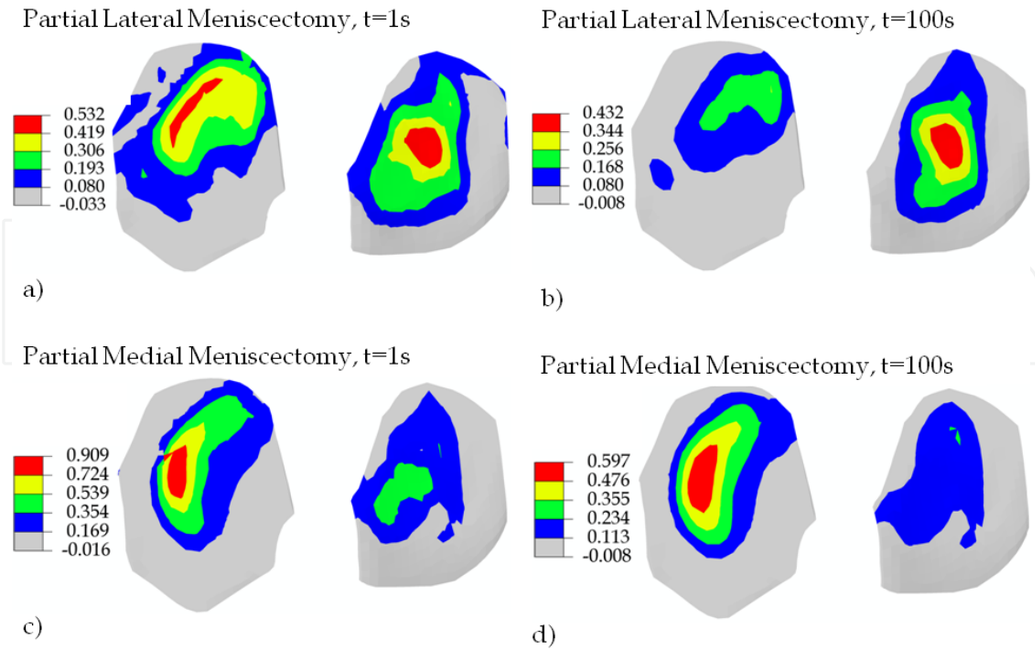

Fig. 8. Fluid pressure (MPa) in the tibial cartilages. (a) and (b) extended lateral meniscectomy; (c) and (d) extended medial meniscectomy. The pressure was obtained for the centroids of the elements. The lateral side is on the right (top view)

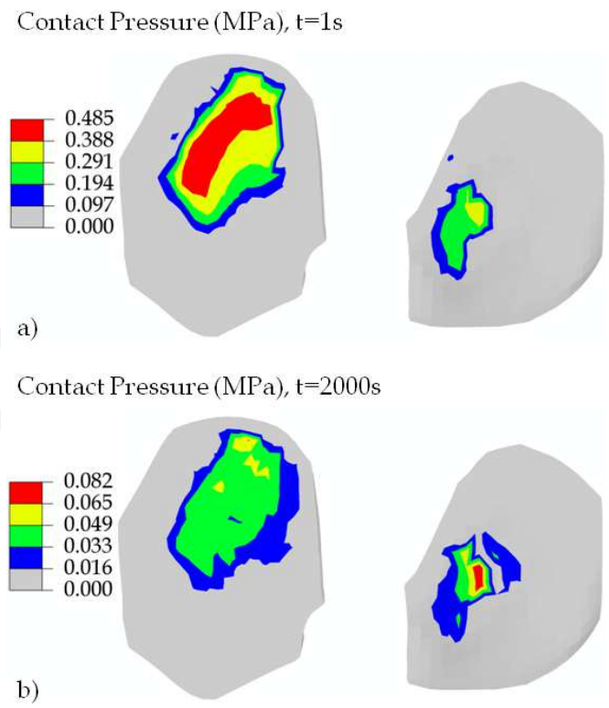

Fig. 9. Contact pressure (MPa) on the articular surface of the tibial cartilages for the case of extended lateral meniscectomy. The lateral side is on the right (top view)

The contact pressures on the articular surfaces are shown in Fig. 9 for the tibial cartilages and Fig. 10 for the femoral cartilage, both for the case of extended lateral meniscectomy. Again, the contact pressures were very low at later stage of relaxation (Figs. 9b and 10b). It was not clear why the maximum contact pressures on the surface (Fig. 9a) were not greater than the maximum fluid pressure within the tissue shown in Fig. 8a. However, it was most likely due to the coarse mesh for the tibial cartilages. There was only one layer of elements for the tibial cartilages, comparing to four layers of elements for the femoral cartilage.

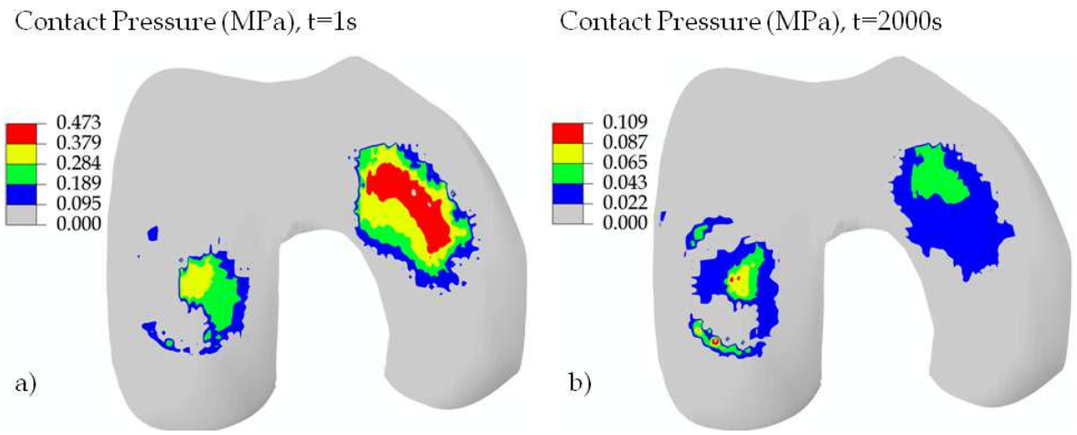

Fig. 10. Contact pressure on the articular surface of the femoral cartilage for the case of extended lateral meniscectomy. The medial condyle is on the right (inferior view)

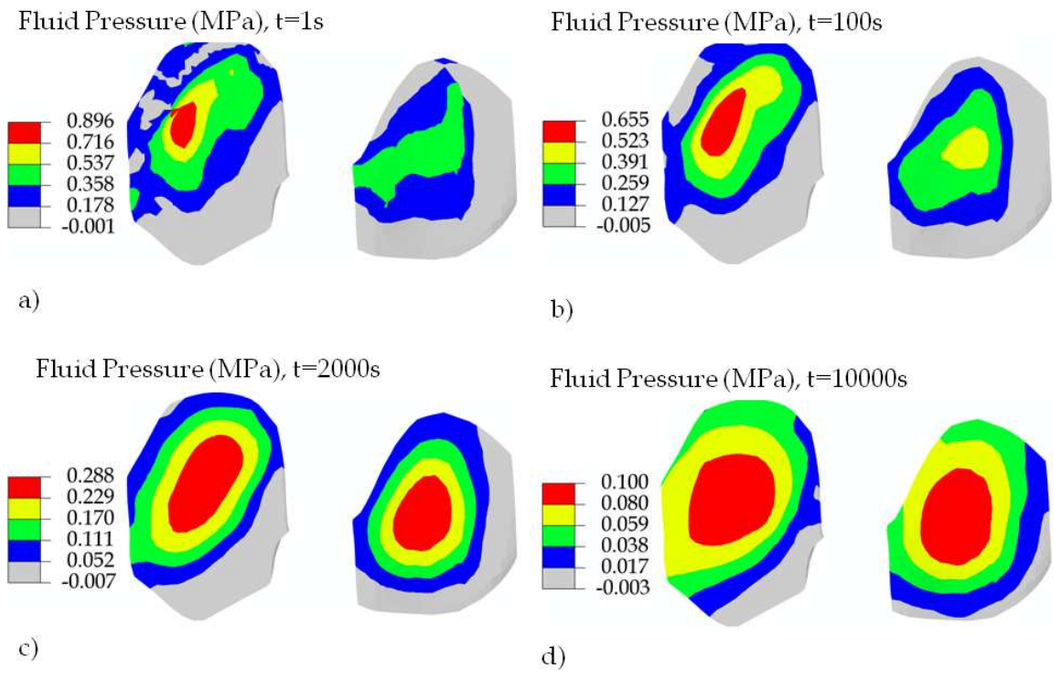

Fig. 11. Fluid pressure in the tibial cartilages for the case of total meniscectomy. The lateral side is on the right and posterior side below (top view)

TOTAL MENISCECTOMY − The fluid pressures in the tibial and femoral cartilages are shown in Figs. 11 and 12, respectively, for the case of total meniscectomy, i.e. when both menisci were removed. The contours here look more in regular shape, possibly because the poorly-shaped meniscal elements were removed. The dissipation of fluid pressure was substantially slowed down by total meniscectomy (Figs. 11 and 12). The peak fluid pressure was the maximum at 1 second. The maximum fluid pressure was still at 32% and 11% of the peak value, respectively, even at 2000 and 10000 seconds (Fig. 11). The medial condyle was more pressurized than the lateral one at 1 second, but the loading was more balanced between the two condyles at 2000 seconds (Fig. 12).

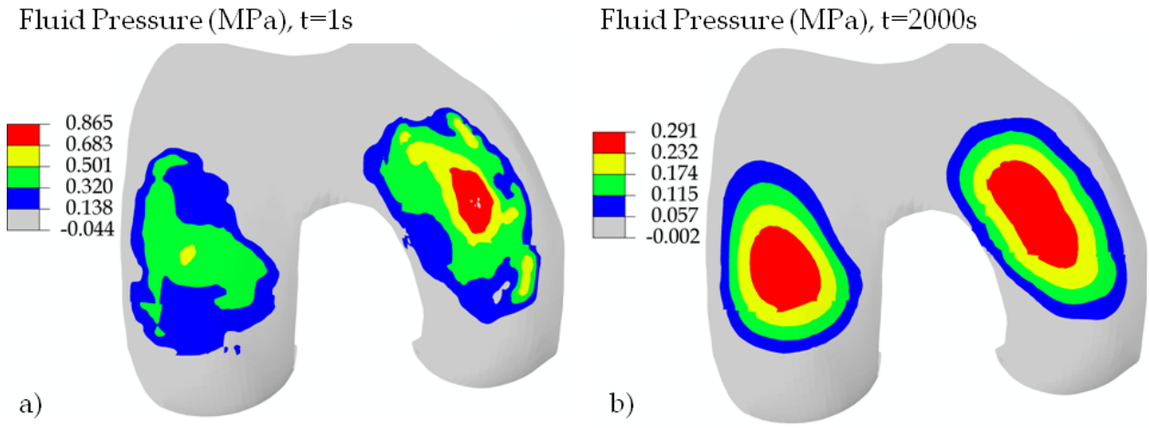

Fig. 12. Fluid pressure in the deep layer of the femoral cartilage for the case of total meniscectomy. The pressure was obtained for the centroids of the elements that were located approximately 3/4 of the depth from the articular surface. The medial condyle is on the right (inferior view)

Comparing to the intact knee, a greater fluid pressure gradient was produced by meniscal removal and it was significant for at least 100 seconds (Fig. 11a,b). Note this was the case of relaxation loading: the maximum compression was constant after 1 second. It was possible that part of the 0.3mm-compression was absorbed by the menisci for the case of the intact knee. The greater pressure gradient was more likely produced by stress concentration.

4. Discussions

The fluid pressures in the cartilaginous tissues and contact pressures between the articulating surfaces were obtained for the normal, partial and total meniscectomized human knees. The constitutive law for the soft tissues was previously developed and numerically incorporated in the commercial finite element software ABAQUS (Li et al., 1999b, 2009). The present results complemented our recent studies, when we simulated 0.1-mm compressive relaxation for the intact knee (Gu and Li, 2011) and 300-N creep loading for the total meniscectomized knee (Kazemi at al., 2011). There were indications that some of our previous results were compatible with limited experimental data available from the literature. Here, we were not able to validate the computational results with more experimental data. However, we saw that the fluid pressure in Fig. 3a was compatible with the contact pressure in Fig. 4a: they had similar distributions but the contact pressure, which was contributed from both the fluid pressure and the tissue matrix, was greater than the

fluid pressure. We also observed that both the maximum fluid and contact pressures occurred at the medial-anterior side (Figs. 3a, 4a, 5a and 6a) (note that Figs. 3 and 4 are top view, while Figs. 5 and 6 are inferior view). These observations indicated reasonable results.

4.1 Significance of fluid pressurization in contact mechanics

In agreement with previous studies, the contact pressure between two articulating surfaces in the knee was predominantly contributed from the fluid pressurization in the cartilaginous tissues, and thus highly time-dependent when joint loadings were applied quickly. The high-pressure regions in the tissues also moved with time (Figs. 2-6, a vs b respectively). These results have not been available from the literature, when the knee joint is modeled as elastic solid (while the fluid phase is not considered).

The fluid pressurization was even more significant in meniscectomized knees. Note that the pressure was also dependent on the types of loadings that were applied on the knee. The fluid pressure lasted much longer with creep loading, as observed in the experiments with tissue explants (Li et al., 2008) and also found in our previous knee modeling (Kazemi et al., 2011).

According to published fibril-reinforced modeling of articular cartilage *in vitro*, the strong fluid pressurization was produced by the nonlinear collagen fiber-reinforcement in the tissues (Li et al., 2003). The collagen fiber orientation and fibrillar properties were particularly considered in the present modeling, which was an important feature of the simulations presented here. These pressure results for the cartilaginous tissues *in situ* may provide additional information on the injury and pathomechanics of the knee joint. For example, collagen degeneration is believed to trigger osteoarthritis. We may use similar modeling to investigate the alteration of the fluid pressure in the knee initiated by collagen generation at a particular site in order to understand the progression of osteoarthritis.

4.2 Effect of meniscectomy on contact mechanics

Meniscectomy caused the pressure increase in the joint (Figs. 12 vs 5), and also slowed down the fluid pressure dissipation during relaxation: the maximum fluid pressure at 2000 second was reduced to 9.3% of the peak value at 1 second for the intact knee (Figs. 5b vs 5a), but to 33.6% for the case of total meniscectomy (Figs. 12b vs 12a). This result may explain the clinical observation that meniscectomy caused stiffness in the knees. However, the alteration in pressure was very minor in the cases of partial meniscectomies, as compared to the total meniscectomy (Figs. 3a, 8a & 11a). This was because the relaxation loading was considered. The effect of partial meniscectomy was more significant in creep than in relaxation as we found in another study using the same computer modeling.

A partial meniscectomy may change the load balance in the knee joint. For the intact knee, the medial side was more pressurized than the lateral side before relaxation (Figs. 3a, 4a, 5a & 6a). A meniscectomy increased the fluid pressure from the normal level. Therefore, the fluid pressure became much higher in the medial side than the lateral side after medial meniscectomy (Fig 8c).

The total meniscectomy was studied previously for the case of creep loading (Kazemi et al., 2011). In that case, the peak fluid pressure in the femoral cartilage at 1 second was at the same level as it here. However, the maximum fluid pressure at 2000 second was only reduced by 20% from the peak pressure in the case of creep, as compared 66% for the present case of relaxation (Fig. 12). Therefore, the clinical implication of total meniscectomy was more significant than the present results have shown, because creep is closer to the physiological loadings than relaxation.

4.3 Numerical convergence, limitations and challenges

In spite of careful control of the solution procedure within the commercial software, there were indeed indications of possible numerical problems. For example, the maximum contact pressure was not greater than the maximum fluid pressure in the femoral cartilage (Figs. 5a vs 6a). This might have been caused by the errors in mesh, especially the coarse meshes for the menisci and tibial cartilages. However, it was also possible that the maximum fluid pressure in the deep layer of the femoral cartilage (Fig. 5a) was supposed to be greater than the maximum contact pressure on the articular surface (Fig. 6a). We did not plot the fluid pressure in the surface layer, because the results there did not precisely agree with the actual contact boundary due to the incapability of applying accurate zero pressure boundary condition around the contact area. This was because the closest boundary applied was determined by the corner nodes of the elements that were closest to the actual contact boundary. These closest nodes did not precisely describe the actual contact boundary due to the coarse mesh used in the simulations. The numerical accuracy of such results can be improved and confirmed later with better meshes when more powerful computers are used. The fluid pressures shown for the deep layers should have negligible influence from the inaccurate fluid pressure boundary conditions.

The main limitations of the present study were the small deformation assumption and the use of non-physiological loadings. The small compression used might not have been sufficient to minimize the influences of the geometrical errors that were introduced by meshing or by the reconstruction of the knee model from MRI data. The simulations were time-consuming even for these simple cases, because of the multiple mechanical contacts involved in the time-dependent problem. We chose these simple cases to start with the research, and will validate these results later with a formulation of large deformation.

Other issues existed such as the poor element aspect ratios and some distorted elements used in the simulations, in order to limit the number of nodes and speed up the solutions. The cartilaginous tissues are very thin (articular cartilage 1-5mm), especially at the inner edge of meniscus (where the thickness is close to zero). Therefore, the 3D finite elements must be very thin and several times wider in other two directions. The issue with aspect ratio can be solved in the future using more computer power, e.g. using computers with dozens of CPUs. However, the issue with distort elements can only be improved. Some distorted elements are unavoidable in order to match the geometry of the tissue, such as the inner edge of the meniscus. Special finite elements could be developed to address this tissue.

It would be challenging to simulate physiological loadings in walking. The computer power never seems to be sufficient. Currently, using a new 6-core computer with 24 GB RAMs, it takes hours to a full day (depending on the meshes used) to run the first second simulation in the loading phase (up to hundreds of times faster in later relaxation and creep phase). Numerical difficulties would also be expected when the contact in the knee is dynamic.

Accurate surface reconstruction is essential for correct modeling of the mechanical contact in the knee joint. For this purpose, we have obtained new MRIs using the 3-Tesla facility at the University MR research centre. Images in both sagittal and coronal planes were obtained for the same knee and will be used to construct precise surfaces and tissue boundaries. We will also determine and minimize the geometrical errors introduced by finite element meshes. We should be able to obtain new results soon.

It is always important to validate the computational results with experimental data. We plan to test the modeling in a few different settings, such as measuring the tissue deformation

with MRI under static compression and cadaveric knee mechanical tests. This is beyond the scope of this chapter.

5. Summary and conclusions

The computer simulations on the mechanical response of human knee joint have been mostly based on the single-phase elastic modeling of the soft tissues. The fluid pressure in the tissues *in situ* has not been available from the literature until our recent publications (Gu and Li, 2011; Kazemi et al., 2011), although the fluid pressurization is believed to play an important role in the mechanical functioning of the joints, and has been studied both theoretically and experimentally for decades at the tissue level. Our recent studies extended the previous fibril-reinforced modeling at the tissue level to the joint level. Compared to most existing knee models from the literature, two major features were added in the present modeling: the fluid flow/pressurization in articular cartilages and menisci, and realistic site-specific fiber orientations in the femoral cartilage and menisci.

The tissue model was previously validated against experimental data under several loading conditions. The constitutive law was numerically incorporated in the commercial software ABAQUS using the option of user-defined material. The meshes for the femoral cartilage were more refined and the fiber orientations there were incorporated using measured split-line pattern from the literature (Below at al., 2002). Coarse meshes (one layer only) were used for the tibial cartilages because our previous focus was on the femoral cartilage. The meshes for the menisci were difficult to be refined because of the wedge shape. Converged solutions were obtained that satisfied desired criteria. However, the pressures in the deep layer of the femoral cartilage might be more reliable than other results.

The present study has shown the importance of the fluid pressurization in the mechanical functions of the normal and repaired human knees. The remainder of the normal tissues can be more pressurized with injuries or repairs in the knee. The site of the repair and the amount of tissues that were lost in injury may be important parameters for the altered mechanical functions of the knee. The present results were obtained for small knee compression which might have been compromised by small errors in surface geometries. However, the modeling can obviously be used to study site-specific cartilage degeneration and injury after large deformation is incorporated.

The present study may also indicate the limitation of previous elastic modeling that did not consider the fluid pressure, which was not explored in the chapter. An independent study, however, showed that the results predicted by elastic models were compromised but could provide certain useful information if the results were interpreted correctly.

6. Acknowledgments

The present study was partially supported by the Natural Sciences and Engineering Research Council (NSERC) of Canada. The second author also received a scholarship from the NSERC Create training program. The knee geometry was reconstructed using MRI data by Drs. Ming Zhang and Jason Cheung at the Hong Kong Polytechnic University in China.

7. References

Adeeb, SM., Ahmed, EYS., Matyas, J., Hart, DA., Frank, CB. & Shrive, NG. (2004). Congruency Effects on Load Bearing in Diarthrodial Joints. *Computer Methods in Biomechanics and Biomedical Engineering*, Vol.7, No.3, pp. 147-157, ISSN 1025-5842

Armstrong, CG., Bahrani, AS. & Gardner DL. (1980). Changes in the Deformational Behavior of Human Hip Cartilage with Age. *Journal of Biomechanical Engineering*, Vol.102, No.3, pp. 214-220, ISSN 0148-0731

Aspden, RM., Yarker, YE. & Hukins, DW. (1985). Collagen Orientations in the Meniscus of the Knee Joint. *Journal of Anatomy*, Vol.140, No.3, pp. 371-380, ISSN 00218782

Ateshian, GA., Lai, WM., Zhu, WB. & Mow, VC. (1994). An Asymptotic Solution for the Contact of Two Biphasic Cartilage Layers. *Journal of Biomechanics*, Vol.27, No.11, pp. 1347-1360, ISSN 0021-9290

Below, S., Arnoczky, SP., Dodds, J., Kooima, C. & Walter, N. (2002). The Split-Line Pattern of the Distal Femur: a Consideration in the Orientation of Autologous Cartilage Grafts. *J Arthroscopic and Related Surgery*, Vol.18, No.6, pp. 613-617, ISSN 0749-8063

Bendjaballah, MZ., Shirazi-Adl, A. & Zukor, DJ. (1995). Biomechanics of the Human Knee Joint in Compression: Reconstruction, Mesh Generation and Finite Element Analysis. *The Knee*, Vol.2, No.2, pp. 69-79, ISSN 0968-0160

Biot, MA. (1941). General Theory of Three Dimensional Consolidation. *Journal of Applied Physics*, Vol.12, No.2, pp. 155-164, ISSN 0021-8979

Biot, MA. (1962). Mechanics of Deformation and Acoustic Propagation in Porous Media. *Journal of Applied Physics*, Vol.33, No.4, pp. 1482-1498, ISSN 0021-8979

Brown, TD. & Singerman, RJ. (1986). Experimental Determination of the Linear Biphasic Constitutive Coefficients of Human Fetal Proximal Femoral Chondroepiphysis. *Journal of Biomechanics*, Vol.19, pp. 597-605, ISSN 0021-9290

Callaghan, JJ., Rosenberg, AG., Rubash HE., Simonian, PT. & Wickiewicz, TL. (2003). *The Adult Knee*. (Vol.I), Lippincott Williams & Wilkins, ISBN 0781732476, Philadelphia

Coletti, JMJ., Akeson, WH. & Woo, SL. (1972). A Comparison of the Physical Behavior of Normal Articular Cartilage and the Arthroplasty Surface. *Journal of Bone and Joint Surgery - Series A*, Vol.54, No.1, pp. 147-160, ISSN 0021-9355

Cheung, JTM., Zhang, M., Leung , AKL. & Fan, YB. (2005). Three-dimensional Finite Element Analysis of the Foot During Standing – A Material Sensitivity Study. *Journal of Biomechannics*, Vol.38, pp. 1045-1054, ISSN 0021-9290

Daniel, DM., Akeson, WH. & O'Connor, JJ. (1990). *Knee Ligaments: Structure, Function, Injury and Repair*. Raven Press, ISBN 0881676055, New York

Dandy, DJ. (1990). The Arthroscopic Anatomy of Symptomatic Meniscal Lesions. *Journal of Bone and Joint Surgery - Series B,* Vol.72, No.4, pp. 628-633, ISSN 0301-620X

Fithian, DC., Kelly, MA. & Mow VC. (1990). Material Properties and Structure-Function Relationships in the Menisci. *Clinical Orthopaedics and Related Research*, Vol.252, pp. 19-31, ISSN 0009-921X

Greis, PE., Bardana, DD., Holmstrom, MC. & Burks, RT. (2002). Meniscal Injury: I. Basic Science and Evaluation. *The Journal of the American Academy of Orthopaedic Surgeons*, Vol.10, No.3, pp. 168-176, ISSN 1067-151X

Grood, ES. & Hefzy, MS. (1982). An Analytical Technique for Modeling Knee Joint Stiffness. Part I: Ligamentous Forces. *Journal of Biomechanical Engineering*, Vol.104, No.4, pp. 330-337, ISSN 0148-0731

Gu, KB. & Li, LP. (2011). A Human Knee Joint Model Considering Fluid Pressure and Fiber Orientation in Cartilages and Menisci. *Medical Engineering and Physics*, Vol.33, No.4, pp. 497-503, ISSN 1350-4533

Haut Donahue, TL., Hull, ML., Rashid, MM. & Jacobs, CR. (2002). A Finite Element Model of the Human Knee Joint for the Study of Tibio-Femoral Contact. *Journal of Biomechanical Engineering,* Vol.124, No.3. pp. 273-280, ISSN 0148-0731

Hayes, WC., Keer, LM., Herrmann, G. & Mockros, LF. (1972). A Mathematical Analysis for Indentation Tests of Articular Cartilage. *Journal of Biomechanics*, Vol.5, No.5, pp. 541-551, ISSN 0021-9290

Hayes, WC. & Mockros, J. (1971). Viscoelastic Properties of Human Articular Cartilage. *Journal of applied physiology*, Vol.31, No.4, pp. 562–568, ISSN 0021-8987

Hirokawa, S. & Tsuruno, R. (2000). Three-Dimensional Deformation and Stress Distribution in an Analytical/Computational Model of the Anterior Cruciate Ligament. *Journal of Biomechanics*, Vol.33, No.9, pp. 1069-1077, ISSN 0021-9290

Kazemi, M., Li, LP., Savard, P. & Buschmann, MD. (2011). Creep Behavior of the Intact and Meniscectomy Knee Joints. *Journal of the Mechanical Behavior of Biomedical Materials*, Vol.4, No.7, 1351-1358, doi:10.1016/j.jmbbm.2011.05.004, ISSN 1751-6161

Kempson, GE., Freeman, MAR. & Swanson, SAV. (1971). The Determination of a Creep Modulus for Articular Cartilage from Indentation Tests on the Human Femoral Head. *Journal of Biomechanics,* Vol.4, No.4, pp. 239-250, ISSN 0021-9290

Kurosawa, H., Fukubayashi, T. & Nakajima, H. (1980). Load-Bearing Mode of the Knee Joint: Physical Behavior of the Knee Joint with or Without Menisci. *Clinical Orthopaedics and Related Research*, Vol.149, pp. 283-290, ISSN 0009-921X

Lai, WM., Mow, VC. & Roth, V. (1981). Effects of Non-Linear Strain-Dependent Permeability and Rate of Compression on the Stress Behaviour of Articular Cartilage. *Journal of Biomechanical Engineering,* Vol.103, No.2, pp. 61-66, ISSN 0148-0731

Lanir, Y. (1987). Biorheology and Fluid Flux in Swelling Tissues. II. Analysis of Unconfined Compressive Response of Transversely Isotropic Cartilage Disc. *Biorheology*, Vol.24, pp. 189-205, 0006-355X

Li, LP., Buschmann, MD. & Shirazi-Adl, A. (2003). Strain Rate Dependent Stiffness of Articular Cartilage in Unconfined Compression. *Journal of Biomechanical Engineering,* Vol.125, No.2, pp. 161-168, ISSN 0148-0731

Li, LP, Cheung, JTM., & Herzog W (2009). Three-dimensional Fibril-Reinforced Finite Element Model of Articular Cartilage. *Medical & Biological Engineering & Computing*, Vol.47, pp. 607-615, ISSN 0140-0118

Li, G., Gil, J., Kanamori, A. &Woo, SL. (1999a). A Validated Three-Dimensional Computational Model of a Human Knee Joint. *Journal of Biomechanical Engineering*, Vol.121, No.6, pp. 657-662, ISSN 0148-0731

Li, LP. & Gu, KB. (2011). Reconsideration on the Use of Elastic Models to Predict the Instantaneous Load Response of the Knee Joint. *Proceedings of the Institution of Mechanical Engineers, Part H: Journal of Engineering in Medicine*, ISSN 0954-4119. In press, DOI: 10.1177/0954411911412464

Li, LP. & Herzog, W. (2004). Strain-Rate Dependence of Cartilage Stiffness in Unconfined Compression: The Role of Fibril Reinforcement versus Tissue Volume Change in Fluid Pressurization. *Journal of Biomechanics,* Vol.37, No.3, pp. 375-382, ISSN 0021-9290

Li, LP., Korhonen, RK., Iivarinen, J., Jurvelin, JS. & Herzog, W. (2008). Fluid Pressure Driven Fibril Reinforcement in Creep and Relaxation Tests of Articular Cartilage. *Medical Engineering & Physics*, Vol.30, No.2, pp. 182-189, ISSN 1350-4533

Li, LP., Soulhat, J., Buschmann, MD. & Shirazi-Adl, A. (1999b). Non-Linear Analysis of Cartilage in Unconfined Ramp Compression Using a Fibril Reinforced Poroelastic Model. *Clinical Biomechanics*, Vol.14, No.9, pp. 673-682, ISSN 0268-0033

Miller, K. (1998). Modelling Soft Tissue using Biphasic Theory – A Word of Caution. *Computer Methods in Biomechanics and Biomedical Engineering*, Vol.1, pp. 261-263, ISSN 1025-5842

Mow, VC. & Ratcliffe, A. (1990). *Biomechanics of Diarthrodial Joints.* Springer, ISBN 0387973796, New York

Mow, VC., Kuei, SC., Lai, WM. & Armstrong CG. (1980). Biphasic Creep and Stress Relaxation of Articular Cartilage in Compression: Theory and Experiments. *Journal of Biomechanical Engineering,* Vol.102, No.1, pp. 73-84, ISSN 0148-0731

Mow, VC., Ateshian, GA. & Spilker, RL. (1993). Biomechanics of Diarthrodial Joints: A Review of Twenty Years of Progress. *Journal of Biomechanical Engineering,* Vol.115, No.4B, pp. 460-467, ISSN 0148-0731

Nowinski, JL. (1971). Bone Articulations as Systems of Poroelastic Bodies in Contact. *AIAA Journal*, Vol.9, pp. 62-69, ISSN 0001-1452

Nowinski, JL. (1972). Stress Concentrations Around a Cylindrical Cavity in Bone Treated as a Poroelastic Body. *Acta Mechanica*, Vol.13, pp. 281-292, ISSN 0001-5970

Nowinski, JL. & Davis, CF. (1970). A model of the Human Skull as a Poroelastic Spherical Shell Subjected to a Quasistatic Load. *Mathematical Biosciences*, Vol.8, pp. 397-416, ISSN 0025-5564

Nowinski, JL. & Davis, CF. (1972). The Flexure and Torsion of Bones Viewed as Anisotropic Poroelastic Bodies. *International Journal of Engineering Science*, Vol.10, pp. 1063-1079, ISSN 0020-7225

Oloyede, A., Flachsmann R., & Broom ND. (1992). The Dramatic Influence of Loading Velocity on the Compressive Response of Articular Cartilage. *Connective Tissue Research*, Vol.27, pp. 211-244, ISSN 0300-8207

Parsons, JR. & Black J. (1977). The Viscoelastic Shear Behavior of Normal Rabbit Articular Cartilage. *Journal of Biomechanics*, Vol.10, No.1, pp. 21-29, ISSN 0021-9290

Peña, E., Calvo, B., Martínez, MA. & Doblaré, M. (2008). Computer Simulation of Damage on Distal Femoral Articular Cartilage after Meniscectomies. *Computers in Biology and Medicine,* Vol.38, No.1, pp. 69-81, ISSN 0010-4825

Peña, E., Calvo, B., Martínez, MA. & Palanca D, Doblaré M. (2005). Finite Element Analysis of the Effect of Meniscal Tears and Meniscectomies on Human Knee Biomechanics. *Clinical Biomechanics*, Vol.20, No.5, pp. 498-507, ISSN 0268-0033

Peña, E., Calvo, B., Martínez, MA. & Doblaré, M. (2006). A Three-Dimensional Finite Element Analysis of the Combined Behavior of Ligaments and Menisci in the Healthy Human Knee Joint. *Journal of Biomechanics,* Vol.39, No.9, pp. 1686-1701, ISSN 00219290

Penrose, JM., Holt, GM., Beaugonin, M. & Hose, DR. (2002). Development of an Accurate Three-Dimensional Finite Element Knee Model. *Computer Methods in Biomechanics and Biomedical Engineering*, Vol.5, No.4, pp. 291-300, ISSN 1025-5842

Pérez del Palomar, A. & Doblaré, M. (2007). An Accurate Simulation Model of Anteriorly Displaced TMJ Discs with and Without Reduction. *Medical Engineering and Physics*, Vol.29, No.2, pp. 216-226, ISSN 1350-4533

Schanz, M. & Diebels, S. (2003). A Comparative Study of Biot's Theory and the Linear Theory of Porous Media for Wave Propagation Problems. *Acta Mechanica*, Vol.161, pp. 213-235, ISSN 0001-5970

Shirazi, R., Shirazi-Adl, A. & Hurtig, M. (2008). Role of Cartilage Collagen Fibrils Networks in Knee Joint Biomechanics Under Compression. *Journal of Biomechanics,* Vol.41, No.16, pp. 3340-3348, ISSN 0021-9290

Shirazi, R. & Shirazi-Adl, A. (2009). Analysis of Partial Meniscectomy and ACL Reconstruction in Knee Joint Biomechanics Under a Combined Loading. *Clinical Biomechanics,* Vol.24, No.9, pp. 755-761, ISSN 02680033

Simon, BR. (1992). Multiphasic Poroelastic Finite Element Models for Soft Tissue Structures. *Applied Mechanics Riviews*, Vol.45, No.6, pp. 191-218, ISSN 0003-6900

Soulhat, J., Buschmann, MD. & Shirazi-Adl, A. (1999). A Fibril-Network-Reinforced Biphasic Model of Cartilage in Unconfined Compression. *Journal of Biomechanical Engineering,* Vol.121, No.3, pp. 340-347, ISSN 0148-0731

Spilker, RL., Donzelli, PS. & Mow, VC. (1992). A Transversely Isotropic Biphasic Finite Element Model of the Meniscus. *Journal of Biomechanics,* Vol.25, No.9, pp. 1027-1045, ISSN 00219290

Suggs, J., Wang, C. & Li, G. (2003). The Effect of Graft Stiffness on Knee Joint Biomechanics After ACL Reconstruction- a 3D Computational Simulation. *Clinical Biomechanics*, Vol.18, No.1, pp. 35-43, ISSN 0268-0033

Suh, JK., Spilker, RL. & Holmes, MH. (1991). A Penalty Finite Element Analysis for Nonlinear Mechanics of Biphasic Hydrated Soft Tissue under Large Deformation. *International Journal for Numerical Methods in Engineering,* Vol.32, No.7, pp. 1411-1439, ISBN 1097-0207

Swanson, SAV. (1979). Friction, Wear and Lubrication. In: *Adult Articular Cartilage*, MAR. Freeman, (Ed.), 415-457, Pitman Medical, ISBN 039758248X, London, UK

Walker, PS. & Erkman, MJ. (1975). The Role of the Menisci in Force Transmission Across the Knee. *Clinical Orthopaedics and Related Research,* Vol.109, pp. 184-192, ISSN 0009-921X

Walker, PS. & Hajek, JV. (1972). The Load-Bearing Area in the Knee Joint. *Journal of Biomechanics,* Vol.5, No.6, pp. 581-589, ISSN 0021-9290

Wilson, W., van Donkelaar, CC., van Rietbergen, B., Ito, K. & Huiskes, R. (2004). Stresses in the Local Collagen Network of Articular Cartilage: a Poroviscoelastic Fibril-Reinforced Finite Element Study. *Journal of Biomechanics,* Vol.37, No.3, pp. 357-366, ISSN 0021-9290

Woo, SL., Akeson, WH. & Jemmott, GF. (1976). Measurements of Nonhomogeneous, Directional Mechanical Properties of Articular Cartilage in Tension. *Journal of Biomechanics,* Vol.9, No.12, pp. 785-791, ISSN 0021-9290

Wu, JZ., Herzog, W. & Epstein, M. (1998). Evaluation of the Finite Element Software ABAQUS for Biomechanical Modelling of Biphasic Tissues. *Journal of Biomechanics,* Vol.31, pp. 165-169, ISSN 0021-9290

Yang, N., Nayeb-Hashemi, H., & Canavan, PK. (2009). The Combined Effect of Frontal Plane Tibiofemoral Knee Angle and Meniscectomy on the Cartilage Contact Stresses and Strains. *Annals of Biomedical Engineering,* Vol.37, No.11, pp. 2360-2372, ISSN 00906964

Zielinska, B., & Donahue, TL. (2006). 3D Finite Element Model of Meniscectomy: Changes in Joint Contact Behavior. *Journal of Biomechanical Engineering,* Vol.128, No.1, pp. 115-123, ISNN 01480731

Other Related Publications From the Authors

Li, LP., Soulhat, J., Buschmann, MD. & Shirazi-Adl, A. (1999). Non-Linear Analysis of Cartilage in Unconfined Ramp Compression Using a Fibril Reinforced Poroelastic Model. *Clinical Biomechanics*, Vol.14, No.9, pp. 673-682, ISSN 0268-0033

Li, LP., Buschmann, MD. & Shirazi-Adl, A. (2000). A Fibril Reinforced Nonhomogeneous Poroelastic Model for Articular Cartilage: Inhomogeneous Response in Unconfined Compression. *Journal of Biomechanics*, Vol.33, No.12, pp. 1533-1541, ISSN 00219290

Li, LP., Buschmann, MD. & Shirazi-Adl, A. (2001). The Asymmetry of Transient Response in Compression vs Release for Cartilage in Unconfined Compression. *ASME Journal of Biomechanical Engineering,* Vol.123, No. 5, pp. 519-522, ISSN 01480731

Li, LP., Buschmann, MD. & Shirazi-Adl, A. (2002). The Role of Fibril Reinforcement in the Mechanical Behavior of Cartilage. *Biorheology*, Vol.39, Nos. 1-2, pp. 89-96, ISSN 0006355X

Li, LP., Shirazi-Adl, A. & Buschmann, MD. (2002). Alterations in Mechanical Behavior of Articular Cartilage due to Changes in Depth Varying Material Properties - A Nonhomogeneous Poroelastic Model Study. *Computer Methods in Biomechanics and Biomedical Engineering,* Vol.5, No. 1, pp. 45-52, ISSN 10255842

Li, LP., Shirazi-Adl, A. & Buschmann, MD. (2003). Investigation of Mechanical Behavior of Articular Cartilage by Fibril Reinforced Poroelastic Models. *Biorheology,* Vol.40, Nos. 1-3, pp. 227-233, ISSN 0006355X

Li, LP., Buschmann, MD. & Shirazi-Adl, A. (2003). Strain Rate Dependent Stiffness of Articular Cartilage in Unconfined Compression. *Journal of Biomechanical Engineering,* Vol.125, No.2, pp. 161-168, ISSN 0148-0731

Li, LP., & Herzog, W. (2004). Strain-Rate Dependence of Cartilage Stiffness in Unconfined Compression: The Role of Fibril Reinforcement versus Tissue Volume Change in Fluid Pressurization. *Journal of Biomechanics,* Vol.37, No.3, pp. 375-382, ISSN 0021-9290

Li, LP., & Herzog, W. (2004). The Role of Viscoelasticity of Collagen Fibers in Articular Cartilage: Theory and Numerical Formulation. *Biorheology, Vol.*41, Nos. 3-4, pp. 181-194, ISSN 0006355X

Li, LP., Herzog, W., Korhonen, RK. & Jurvelin, JS. (2005). The Role of Viscoelasticity of Collagen Fibers in Articular Cartilage: Axial Tension versus Compression. *Medical Engineering & Physics*, Vol.27, No.1, pp. 51-57, ISSN 13504533

Li, LP., & Herzog, W. (2005). Electromechanical Response of Articular Cartilage in Indentation - Considerations on the Determination of Cartilage Properties during Arthroscopy. *Computer Methods in Biomechanics and Biomedical Engineering*, Vol.8, No.2, pp. 83-91, ISSN 10255842

Li, LP., & Herzog, W. (2006). Arthroscopic Evaluation of Cartilage Degeneration using Indentation Testing - Influence of Indenter Geometry. *Clinical Biomechanics*, Vol.21, No. 4, pp. 420-426, ISSN 02680033

Li, LP., Korhonen, RK., Iivarinen, J., Jurvelin, JS. & Herzog, W. (2008). Fluid Pressure Driven Fibril Reinforcement in Creep and Relaxation Tests of Articular Cartilage. *Medical Engineering & Physics*, Vol.30, No.2, pp. 182-189, ISSN 1350-4533

Li, LP, Cheung, JTM., & Herzog W (2009). Three-dimensional Fibril-Reinforced Finite Element Model of Articular Cartilage. *Medical & Biological Engineering & Computing*, Vol.47, pp. 607-615, ISSN 0140-0118

Gu, KB. & Li, LP. (2011). A Human Knee Joint Model Considering Fluid Pressure and Fiber Orientation in Cartilages and Menisci. *Medical Engineering and Physics*, Vol.33, No.4, pp. 497-503, ISSN 1350-4533

Kazemi, M., Li, LP., Savard, P. & Buschmann, MD. (2011). Creep Behavior of the Intact and Meniscectomy Knee Joints. *Journal of the Mechanical Behavior of Biomedical Materials*, Vol.4, No.7, 1351-1358, ISSN 1751-6161

Li, LP. & Gu, KB. (2011). Reconsideration on the Use of Elastic Models to Predict the Instantaneous Load Response of the Knee Joint. *Proceedings of the Institution of Mechanical Engineers, Part H: Journal of Engineering in Medicine*, Vol.225, pp. 888-896, ISSN 0954-4119

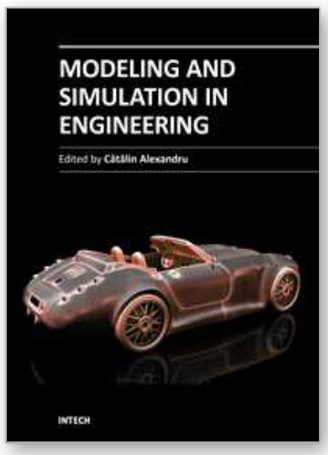

Modeling and Simulation in Engineering
Edited by Prof. Catalin Alexandru

ISBN 978-953-51-0012-6
Hard cover, 298 pages
Publisher InTech
Published online 07, March, 2012
Published in print edition March, 2012

This book provides an open platform to establish and share knowledge developed by scholars, scientists, and engineers from all over the world, about various applications of the modeling and simulation in the design process of products, in various engineering fields. The book consists of 12 chapters arranged in two sections (3D Modeling and Virtual Prototyping), reflecting the multidimensionality of applications related to modeling and simulation. Some of the most recent modeling and simulation techniques, as well as some of the most accurate and sophisticated software in treating complex systems, are applied. All the original contributions in this book are jointed by the basic principle of a successful modeling and simulation process: as complex as necessary, and as simple as possible. The idea is to manipulate the simplifying assumptions in a way that reduces the complexity of the model (in order to make a real-time simulation), but without altering the precision of the results.

INTECH
open science | open minds

InTech Europe
University Campus STeP Ri
Slavka Krautzeka 83/A
51000 Rijeka, Croatia
Phone: +385 (51) 770 447
Fax: +385 (51) 686 166
www.intechopen.com

InTech China
Unit 405, Office Block, Hotel Equatorial Shanghai
No.65, Yan An Road (West), Shanghai, 200040, China
中国上海市延安西路65号上海国际贵都大饭店办公楼405单元
Phone: +86-21-62489820
Fax: +86-21-62489821

IntechOpen